ELSEVIER

Biophysical Chemistry 104 (2003) 573–589

Biophysical Chemistry

www.elsevier.com/locate/bpc

A kinetic model of the cyclin E/Cdk2 developmental timer in *Xenopus laevis* embryos

Andrea Ciliberto, Matthew J. Petrus, John J. Tyson, Jill C. Sible*

Biology Department, Virginia Polytechnic Institute and State University, Blacksburg, VA 24061-0406, USA

Received 20 December 2002; received in revised form 10 March 2003; accepted 10 March 2003

Abstract

Early cell cycles of *Xenopus laevis* embryos are characterized by rapid oscillations in the activity of two cyclin-dependent kinases. Cdk1 activity peaks at mitosis, driven by periodic degradation of cyclins A and B. In contrast, Cdk2 activity oscillates twice per cell cycle, despite a constant level of its partner, cyclin E. Cyclin E degrades at a fixed time after fertilization, normally corresponding to the midblastula transition. Based on published data and new experiments, we constructed a mathematical model in which: (1) oscillations in Cdk2 activity depend upon changes in phosphorylation, (2) Cdk2 participates in a negative feedback loop with the inhibitory kinase Wee1; (3) cyclin E is cooperatively removed from the oscillatory system; and (4) removed cyclin E is degraded by a pathway activated by cyclin E/Cdk2 itself. The model's predictions about embryos injected with Xic1, a stoichiometric inhibitor of cyclin E/Cdk2, were experimentally validated.
© 2003 Elsevier Science B.V. All rights reserved.

Keywords: Cyclin E; Cyclin-dependent kinase 2 (Cdk2); Wee1; Xic1; Midblastula transition; Mathematical model

1. Introduction

The chromosome replication–division cycle of cell-free extracts derived from *Xenopus laevis* eggs has been well characterized by rigorous experimentation [1–12] and mathematical modeling [13–16]. In the egg extract system, the chromosome cycle is driven by oscillations in the activity of M-phase promoting factor (MPF), a dimer of a catalytic subunit, Cdk1, and a regulatory subunit, cyclin A1 or B [3]. Oscillations in MPF activity depend upon a negative feedback loop in which active MPF promotes degradation of mitotic cyclins [12,17]. MPF activity is also modulated by inhibitory phosphorylation on threonine 14 and tyrosine 15. These sites are phosphorylated by Wee1 and Myt1 [5,6], and dephosphorylated by Cdc25 [7,8]. The autocatalytic nature of MPF activation [18–20] depends upon positive feedback loops, whereby MPF activates Cdc25 [11,21] and inhibits Wee1 [5].

Cell cycle controls in intact, developing *Xenopus* embryos present additional experimental and theo-

Abbreviations: Cdk, cyclin-dependent kinase; MPF, M-phase promoting factor; MBT, midblastula transition; ODE, ordinary differential equation; pf, post-fertilization.

*Corresponding author. Tel.: +1-540-231-1842; fax: +1-540-231-9307.

E-mail addresses: siblej@vt.edu (J.C. Sible), ancilibe@vt.edu (A. Ciliberto), mapetrus@vt.edu (M.J. Petrus), tyson@vt.edu (J.J. Tyson).

0301-4622/03/$ - see front matter © 2003 Elsevier Science B.V. All rights reserved.
doi:10.1016/S0301-4622(03)00060-7

retical challenges. After fertilization, the egg and sperm nuclei undergo DNA replication, nuclear fusion and the first mitotic division. The next 11 embryonic cell cycles are rapid, synchronous oscillations between DNA replication and mitosis, lacking intervening gap phases, cell growth and cell cycle checkpoints. After the 12th division, the *Xenopus* embryo undergoes the midblastula transition (MBT), when cells become motile, embryonic transcription begins and the cell cycle acquires the gap phases and checkpoints of a typical somatic cell [22,23].

The mechanisms of 'cell cycle remodeling' [24] are not fully understood, but recent evidence suggests that remodeling depends in part on a maternal developmental timer driven by oscillations in the activity of cyclin E/Cdk2 [25]. During cleavage cycles 2–12 in the frog, the cyclin E level is constant, while cyclin E-associated kinase activity (cyclin E/Cdk2) oscillates twice per cell cycle [25,26]. Cyclin E/Cdk2 activity promotes DNA replication [27,28] and is essential for centrosome duplication [29,30]. At the MBT, maternally supplied cyclin E is degraded [25,26,31,32] and Cdk2 activity declines [25], coincident with remodeling of the cell cycle. Maternal cyclin E mRNA disappears some hours later [32].

Injection of embryos with Δ34Xic1 (a recombinant, truncated form of the cyclin-dependent kinase (Cdk) inhibitor, Xic1) specifically inhibits cyclin E/Cdk2, causes a 25% increase in interdivision time, and delays both the MBT (zygotic transcription) and the degradation of cyclin E until approximately the correct nucleocytoplasmic ratio [25]. Although this observation suggests that cyclin E degradation is causally related to the MBT, the two events can be dissociated. Cycloheximide treatment (which inhibits protein synthesis) blocks cell division and the MBT, but does not prevent cyclin E degradation. Nor does α-amanitin treatment (which blocks zygotic transcription at the MBT) prevent cyclin E degradation [25]. Furthermore, oscillations in cyclin E/Cdk2 also occur independently of protein synthesis, the nucleocytoplasmic ratio and embryonic transcription [25].

We have built a mathematical model of the cyclin E/Cdk2 developmental timer that describes both the oscillations in Cdk2 activity and the abrupt destruction of cyclin E coincident with the MBT. The model was constructed along the same lines as the Novak–Tyson model of MPF oscillations in frog egg extracts [13], taking into account the similarities and differences between cyclin B/Cdk1 regulation and cyclin E/Cdk2 regulation. For both Cdk1 and Cdk2, there are no abundant Cdk inhibitors expressed during this time [33]; hence, oscillations are due to either periodic synthesis and degradation of cyclin partners, or periodic phosphorylation and dephosphorylation of kinase subunits (or both). Pre-MBT oscillations of Cdk1 activity are driven by periodic cyclin degradation [34], but pre-MBT oscillations of Cdk2 activity are not [25]. Although early reports indicated no periodic tyrosine phosphorylation of either Cdk1 or Cdk2 until the MBT [26,35], subsequent studies with a sensitive antibody have detected periodic tyrosine phosphorylation of a Cdk in pre-MBT *Xenopus* embryos [36]. Furthermore, Cdk2 activity is regulated in cell-free egg extracts by such phosphorylation events [37]. Therefore, if oscillations in Cdk2 activity are generated by a negative feedback loop (as for Cdk1), the inhibitory phosphorylation state of Cdk2 (rather than cyclin level) is the likely position of the negative feedback.

A second important distinction between the regulation of Cdk1 and Cdk2 activity is the rapid destruction of cyclin E at the MBT. Because the only manipulation known to delay the degradation of cyclin E is to inhibit Cdk2 activity directly [25], we propose that degradation of cyclin E is intrinsically dependent on Cdk2 activity.

Based on the experimental literature, we developed a mathematical model to describe the oscillations in cyclin E/Cdk2 activity and the abrupt degradation of cyclin E at the MBT in the intact *Xenopus* embryo. New experiments were performed to help construct the model. The model should provide a framework around which to design future experiments that will specify the details of a revised, second-generation model.

2. Experimental methods

2.1. Maintenance and manipulation of embryos

Eggs from wild-type *Xenopus laevis* (*Xenopus* Express) were fertilized in vitro, dejellied in 2% cysteine in 0.1× MMR (0.5 mM HEPES, pH 7.8, 10 mM NaCl, 0.2 mM KCl, 0.1 mM $MgSO_4$, 0.2 mM $CaCl_2$, 0.01 mM EDTA) and maintained in 0.1× MMR. Embryos were collected at stages spanning the MBT and staged according to Nieuwkoop and Faber [38]. In some experiments, fertilized eggs were injected with indicated amounts of glutathione *S*-transferase (GST)-tagged Xic1-C or GST-tagged Δ34Xic1 protein dissolved in Xic1 buffer (20 mM HEPES, pH 7.5, 88 mM NaCl, 20 mM β-mercaptoethanol, 7.5 mM $MgCl_2$, 5% glycerol) at a concentration of 0.08–0.33 mg/ml. As described by Su et al. [39], Xic1-C contains amino acids 97–210 and Δ34Xic1 contains amino acids 25–210 of the Xic1 protein. The Xic1 proteins were gifts of James Maller (Howard Hughes Medical Institute, University of Colorado Health Sciences Center). Microinjected embryos were maintained in 5% Ficoll in 0.1× MMR, and snap-frozen at the time points indicated. Some embryos were also injected with 50 ng of α-amanitin dissolved in H_2O. In some experiments, fertilized eggs were injected with buffer or 15 ng of mRNA encoding luciferase or XChk1 (transcribed in vitro using the mMessage mMachine kit from Ambion), as described elsewhere [40].

2.2. Immunoblotting

Embryos were collected at the times indicated, snap-frozen on dry ice and homogenized in EB buffer (20–30 mM HEPES, pH 7.5, 15 mM $MgCl_2$, 20 mM EGTA, 1 mM dithiothreitol, 1 mM sodium vanadate, 1 mM microcystin, 1 mM phenylmethylsulfonyl fluoride, and 3 μg/ml each leupeptin, pepstatin and chymostatin, with or without 80 mM β-glycerophosphate and 50 mM sodium fluoride). Embryo lysates were resolved by sodium dodecyl sulfate-polyacrylamide gel electrophoresis (SDS-PAGE), transferred to nitrocellulose membranes, and hybridized with antibodies, as previously described [40,41]. The cyclin E antibody was purified from serum provided by Rebecca Hartley (University of New Mexico Health Sciences Center). Xic1 antibodies were generously provided by James Maller (Howard Hughes Medical Institute, University of Colorado Health Sciences Center). To visualize immunoreactive proteins, a horseradish peroxidase-conjugated secondary antibody was hybridized, and chemiluminescence from the secondary antibody was detected with the ECL Plus (Amersham) kit.

2.3. Immunoprecipitation and kinase assays of cyclin/Cdk complexes

Embryos injected at the one-cell stage with 5 ng of Xic-C or Δ34Xic1 were collected at the time indicated, and antibodies against cyclin B or cyclin E were used to immunoprecipitate cyclin B/Cdk1 or cyclin E/Cdk2 complexes, respectively, as described by Kappas et al. [40]. Cyclin antibodies were provided by James Maller (Howard Hughes Institute, University of Colorado Health Sciences Center).

3. Mathematical modeling and computational simulation

Mathematical models of hypothetical molecular mechanisms for regulation of cyclin E/Cdk2 activity were constructed by translating a mechanism into a set of ordinary differential equations (ODEs) by standard principles of biochemical kinetics [42]. The ODEs were then provided as input to XPP-AUT, a simulation and analysis software system, freely downloadable from http://www.math.pitt.edu/~bard/xpp/xpp.html. XPP runs on the UNIX operating system. Parameter values were chosen by trial and error, to fit the basic phenomenological properties of the control system (rapid fluctuations in cyclin E/Cdk2 activity followed by abrupt degradation of cyclin E).

4. Results

4.1. Key assumptions

Based on the experimental evidence summarized in Section 1, a set of assumptions upon which the

mathematical model would be based was developed (Table 1). Some assumptions are well grounded in the experimental literature (assumptions 1–3), others remain to be tested (assumption 4) and several (assumptions 5–7) were tested by us experimentally, as described below.

4.1.1. Reagents that inhibit Cdk2 delay the degradation of cyclin E

A fundamental assumption of our working model is that degradation of cyclin E at the MBT results from a cooperative transition in cyclin E/Cdk2 forms. This assumption is based upon published studies demonstrating that cyclin E is degraded at a fixed time post-fertilization, independent of protein synthesis (hence, independent of Cdk1 activity, which requires continued synthesis of mitotic cyclins A and B), cell number, the nucleocytoplasmic ratio and zygotic transcription [25,32]. Furthermore, the only manipulation known to alter the timing of cyclin E degradation is microinjection of Δ34Xic1, a recombinant protein that specifically inhibits Cdk2 but not Cdk1 activity [25]. Because Δ34Xic1 delays the degradation of cyclin E, it seemed likely that the timing mechanism for cyclin E degradation depends upon cyclin E/Cdk2 activity itself.

If this assumption were correct, then other reagents that interfere with cyclin E/Cdk2 activity should also block or delay the degradation of cyclin E. Expression of exogenous XChk1 in *Xenopus* embryos inhibits both Cdk1 and Cdk2 activity [40]; therefore, expression of XChk1 should also block or delay the degradation of cyclin E. To test this prediction, embryos were injected with 15 ng of mRNA encoding FLAG-tagged XChk1. Negative control embryos were injected with buffer or 15 ng of mRNA encoding FLAG-tagged luciferase. Embryos were collected at the times indicated and analyzed for cyclin E content by immunoblotting (Fig. 1). Analogous to embryos injected with Δ34Xic1, cyclin E degradation was delayed in embryos overexpressing XChk1 compared to both buffer (Fig. 1) and luciferase controls (not shown), supporting the hypothesis that timing of cyclin E degradation depends directly on Cdk2 activity.

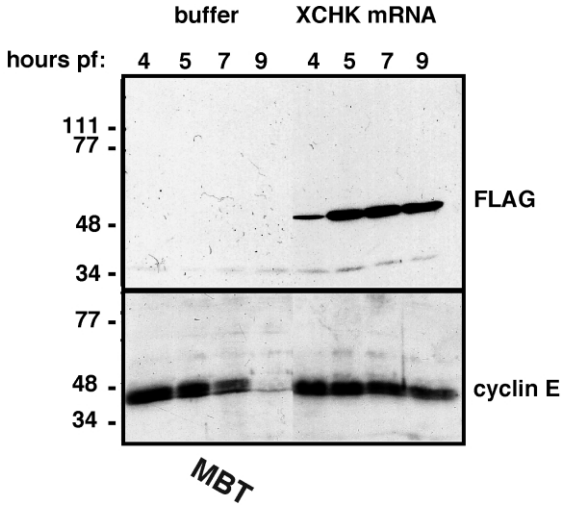

Fig. 1. Expression of XChk1 delays the degradation of cyclin E in *Xenopus* embryos. Embryos were injected with buffer or 15 ng of mRNA encoding XChk1. Embryos were collected at the time points indicated and analyzed for cyclin E protein content. The migration of molecular weight standards in kDa is indicated. In other experiments, control embryos were injected with mRNA encoding luciferase, and the delay in cyclin E degradation was shown to be a specific effect of XChk1 (data not shown).

Table 1
Key assumptions of the cyclin E/Cdk2 kinetic model

1	Constant level of cyclin E	[25,26,31,32]
2	No abundant CKI inhibitor	[33,50]
3	Regulation of Cdk2 activity by phosphorylation	[37,40]
4	Negative feedback loop in Cdk2 oscillations	To be tested
5	Timing of cyclin E degradation linked to Cdk2 activity	[25], Fig. 1
6	No return of Cdk2 activity in Xic-injected embryos	Fig. 2
7	Degradation of cyclin E independent of transcription	[25], Fig. 3

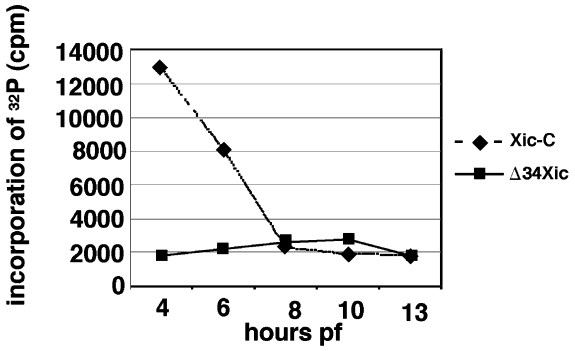

Fig. 2. Cyclin E degradation in Δ34Xic1-treated embryos does not depend upon transient cyclin E/Cdk2 activity. Embryos microinjected with 5 ng of Xic1-C or Δ34Xic1 were collected at the times indicated, cyclin E/Cdk2 was immunoprecipitated and immunoprecipitates were analyzed for histone H1 kinase activity. cpm, counts per minute ^{32}P incorporated into histone H1. Values plotted represent raw cpm − background cpm on gel (1209 cpm). Cyclin B/Cdk1 immunoprecipitates indicated no inhibition of Cdk1 by Δ34Xic1 (not shown).

4.1.2. Cyclin E degradation in Xic1-treated embryos does not depend upon transient cyclin E/Cdk2 activity

When embryos are microinjected with 5 ng of Δ34Xic1, cyclin E/Cdk2 activity is inhibited by more than 90% without inhibition of Cdk1 activity [25]. Intuitively, we would predict that cyclin E degradation would be blocked indefinitely (or until embryos died by necrosis) in Δ34Xic1-injected embryos. However, the degradation of cyclin E does occur, only several hours delayed, when embryos have reached the nucleocytoplasmic ratio of the MBT [25]. This observation challenges the hypothesis that cyclin E degradation is directly linked to cyclin E/Cdk2 activity.

One possible explanation for the eventual degradation of cyclin E in Δ34Xic1-injected embryos is that cyclin E/Cdk2 activity resumes transiently, prior to the degradation of cyclin E, at approximately 9 h post-fertilization (pf). This scenario played a central role in a preliminary mathematical model that simulated the delay in degradation of cyclin E in Δ34Xic1-injected embryos. However, kinase assays performed on embryos injected with Δ34Xic1 detected no transient peak of Cdk2 activity (Fig. 2), even when samples were collected at 30-min intervals (not shown), ruling out this particular model.

4.1.3. Cyclin E degradation in Xic1-treated embryos does not depend upon zygotic transcription

It could be that degradation of cyclin E in embryos injected with Δ34Xic1 is initiated by zygotic transcription at the MBT, since transcription initiates coincident with cyclin E degradation in Δ34Xic1-injected embryos [25]. To determine whether a product of zygotic transcription turned on degradation of maternal cyclin E, independent of cyclin E/Cdk2 activity, embryos were injected with H_2O, α-amanitin (an inhibitor of transcription), Δ34Xic1, or a combination of α-amanitin and Δ34Xic1 (Fig. 3). In embryos injected with H_2O or α-amanitin, cyclin E disappeared between

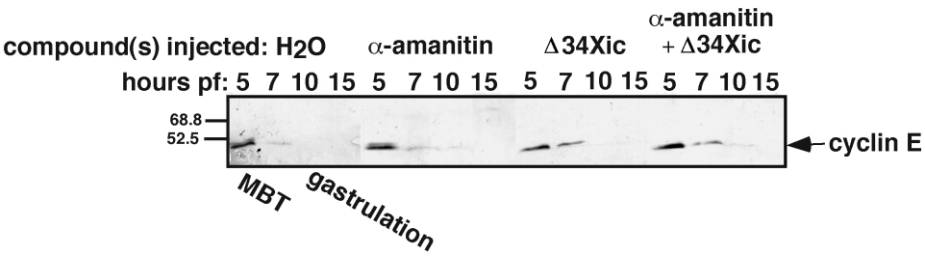

Fig. 3. Zygotic transcription is not required for degradation of cyclin E. Embryos were injected at the one-cell stage with H_2O, 50 ng of α-amanitin, 5 ng of Δ34Xic1, or 50 ng of α-amanitin and 5 ng of Δ34Xic1. Embryos were collected at the indicated times pf and analyzed by immunoblotting for steady-state level of cyclin E protein. The migration of molecular weight standards in kDa is indicated.

5 and 7 h pf, consistent with previous reports that degradation of maternal cyclin E at the MBT does not depend on transcription [25,32]. As predicted [25], degradation of cyclin E was delayed in embryos injected with Δ34Xic1 and was complete by 10 h pf. In embryos injected with both α-amanitin and Δ34Xic1, cyclin E was degraded at the same time as in embryos injected with Δ34Xic1 alone, ruling out the possibility of redundant degradation mechanisms, one dependent upon transcription and the other upon cyclin E/Cdk2 activity. These results indicate that transcription at the MBT is not required for the eventual degradation of cyclin E in embryos lacking cyclin E/Cdk2 activity.

4.2. Kinetic model of the cyclin E/Cdk2 developmental timer

Based on the information summarized in Section 1 and the new data presented in Figs. 1–3, a working model of the cyclin E/Cdk2 control system was developed (Fig. 4). The model is composed of three modules: a negative feedback oscillator, a positive feedback switch and an irreversibly activated pathway for cyclin E degradation.

4.2.1. Negative feedback oscillator

A maternal store of cyclin E combines with free Cdk2 monomers to form active cyclin E/Cdk2 dimers. In the model, we assume cyclin E/Cdk2 dimers can be transformed between an inactive, phosphorylated form (PCdk2:CycE) and an active, non-phosphorylated form (Cdk2:CycE) by the action of a kinase, Wee1, and a phosphatase, Cdc25A. This assumption is based on evidence that Cdk2 is regulated by tyrosine phosphorylation [37,40]. For simplicity, we assume that Cdc25A is present at constant activity in the early embryo, and that Wee1 is periodically activated by cyclin E/Cdk2, indirectly through the action of a hypothetical kinase, Kin. (Cdc25C was not included in the model because dominant-negative Cdc25C does not affect cell cycle length in embryos [36].) In the model, Kin phosphorylates and inactivates Wee1, and cyclin E/Cdk2 phosphorylates and inactivates Kin. These interactions create a delayed negative feedback loop, consisting of three inactivating phosphorylation steps in sequence (Cdk2—|Kin—|Wee1—|Cdk2). (A delayed feedback in which Kin activates Cdc25A would be an alternative possibility.) The parameters in the model are adjusted to create limit cycle oscillations with a period of approximately 15 min (two peaks per mitotic cycle). Because a two-component negative feedback loop (Cdk2—|Wee1—|Cdk2) cannot oscillate [43], we are compelled to introduce the hypothetical kinase (as the simplest case of some process that provides a delay between the actions of Cdk2 and Wee1).

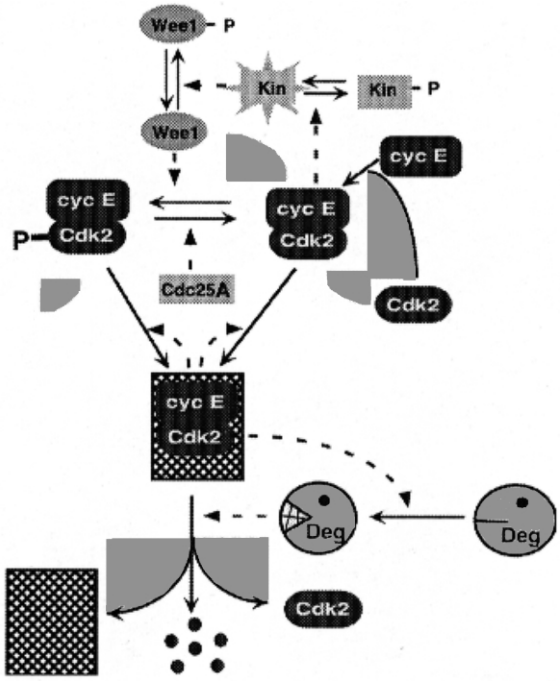

Fig. 4. A theoretical molecular mechanism of the cyclin E/Cdk2 developmental timer was used to construct the mathematical model. The hatched box represents a mechanism for removing cyclin E/Cdk2 from the oscillatory subsystem. 'Deg' represents the cyclin E degradation system, which we assume is activated by the 'removed' form of cyclin E/Cdk2. Notice that the removal step is cooperative, i.e. the more cyclin E/Cdk2 is bound to the hatched box, the faster is the association reaction. A kinase ('Kin') is introduced between cyclin E/Cdk2 and Wee1 to create a time lag in the negative feedback loop.

4.2.2. Positive feedback switch

To model the abrupt degradation of cyclin E at approximately 7 h pf, it is proposed that cyclin E/

Cdk2 is removed from the oscillatory subsystem in a cooperative fashion through a positive feedback loop. Subsequently, the removed form of cyclin E is degraded, probably by the SCF/proteasome pathway. 'Removed' cyclin E/Cdk2 could correspond to a change in phosphorylation state, localization or some other property of cyclin E. Qualitatively, it is predicted that, during the first 7 h of embryonic development, most cyclin E will cycle between active (unphosphorylated) and inactive (Cdk2-phosphorylated) forms. During these oscillations, an increasing fraction of cyclin E/Cdk2 dimers is removed from the oscillating forms, eventually stimulating rapid, cooperative (autocatalytic) removal of cyclin E/Cdk2, which quenches the oscillation.

4.2.3. Cyclin E degradation

After a further delay, the cyclin E degradation machinery ('Deg') activates, and the whole removed pool of cyclin E is degraded. We suppose that Deg is activated by the unphosphorylated form of removed cyclin E/Cdk2 dimers (Cdk2:CycE^{rem}) and that only removed cyclin E is targeted by Deg. Furthermore, the concentration of Cdk2:CycE^{rem} must exceed a certain threshold [Table 2, θ in Eq. (7)] before it can activate Deg. As cyclin E is destroyed, we presume that Deg remains active.

4.2.4. Effect of Δ34Xic1

We assume that (1) Xic1 binds strongly to all forms of cyclin E/Cdk2 and blocks any catalytic activity they may have; nonetheless, (2) Xic1 binding does not interfere with removal of cyclin E/Cdk2. Furthermore, we assume that Xic1 bound to removed forms of cyclin E/Cdk2 is slowly degraded, possibly in association with chromatin [44–46]. As Xic1 is degraded, [Cdk2:CycE^{rem}] increases and subsequently activates cyclin E degradation. Under these assumptions, Xic1 injections are expected to quench oscillations of cyclin E/Cdk2 activity and to delay (but not eliminate) cyclin E degradation.

4.2.5. Further assumptions

The removed forms of cyclin E/Cdk2 are not subject to phosphorylation and dephosphorylation by Wee1 and Cdc25 and do not phosphorylate Kin. These assumptions make the model slightly easier to understand, but they are not necessary. Models in which these assumptions are not made behave very similarly to the model simulated here (not shown).

4.2.6. The model

A mathematical model (the differential equations in Table 2) can be derived from the molecular wiring diagram (Fig. 4) using standard rate laws of biochemical kinetics. Basal parameter values are proposed in Table 3. These values were chosen to reproduce the basic quantitative characteristics of the cyclin E/Cdk2 timer in normal frog embryos. We assume that, at $t=0$ (fertilization, or shortly thereafter), the cyclin E/Cdk2 oscillator is in full swing and no cyclin E is removed from the oscillatory system.

4.3. Numerical simulations and experimental validation: testing the model

4.3.1. The model reproduces the fundamental features of the cyclin E/Cdk2 timer

Fig. 5 presents a numerical solution of the kinetic equations (Table 2) using the basal parameter values proposed for unperturbed embryos (Table 3). The model reproduces the fundamental observations driving this study: (1) cyclin E is a stable protein at first and then rapidly degraded at the MBT [25,32]; and (2) cyclin E/Cdk2 activity oscillates twice per cell cycle before the MBT [25] (Fig. 5a). We did not attempt to model cycle 1, which is longer than cycles 2–12 and involves cyclin E degradation [26].

An appreciation of the regulatory mechanisms behind the oscillations in kinase activity and the abrupt degradation of cyclin E unfolds from graphing the concentrations of the four forms of cyclin E/Cdk2 over time (Fig. 5b). Oscillations in cyclin E/Cdk2 activity prior to the MBT derive from the periodic phosphorylation and dephosphorylation of Cdk2, as a consequence of the negative feedback loop with Wee1. As removed dimers accumulate, Deg is activated and removed cyclin E is degraded.

Because no steps in the model (Fig. 4) involve protein synthesis, the model is consistent with the fact that oscillations in cyclin E/Cdk2 activity [25] and disappearance of cyclin E at a fixed time

Table 2
Differential equations describing the model in Fig. 3

1	$\frac{d}{dt}[\text{Cdk2:CycE}] = -k_{\text{wee}}[\text{Wee1*}][\text{Cdk2:CycE}] + k_{25A}[\text{PCdk2:CycE}] - k_{\text{on}}\phi[\text{Cdk2:CycE}] + k_{\text{off}}[\text{Cdk2:CycE}^{\text{rem}}] - k_{\text{assoc}}[\text{Xic}][\text{Cdk2:CycE}] + k_{\text{dissoc}}[\text{Xic:Cdk2:CycE}]$
2	$\frac{d}{dt}[\text{PCdk2:CycE}] = +k_{\text{wee}}[\text{Wee1*}][\text{Cdk2:CycE}] - k_{25A}[\text{PCdk2:CycE}] - k_{\text{on}}\phi[\text{PCdk2:CycE}] + k_{\text{off}}[\text{PCdk2:CycE}^{\text{rem}}] - k_{\text{assoc}}[\text{Xic}][\text{PCdk2:CycE}] + k_{\text{dissoc}}[\text{Xic:PCdk2:CycE}]$
3	$\frac{d}{dt}[\text{Wee1*}] = +\frac{k_{\text{wact}}([\text{Wee1}_{\text{total}}] - [\text{Wee1*}])}{J_{\text{wact}} + [\text{Wee1}_{\text{total}}] - [\text{Wee1*}]} - \frac{k_{\text{winact}}[\text{Kin*}][\text{Wee1*}]}{J_{\text{winact}} + [\text{Wee1*}]}$
4	$\frac{d}{dt}[\text{Kin*}] = +\frac{k_{\text{iact}}(1 - [\text{Kin*}])}{J_{\text{iact}} + 1 - [\text{Kin*}]} - \frac{k_{\text{iinact}}[\text{Cdk2:CycE}][\text{Kin*}]}{J_{\text{iinact}} + [\text{Kin*}]}$
5	$\frac{d}{dt}[\text{Cdk2:CycE}^{\text{rem}}] = +k_{\text{on}}\phi[\text{Cdk2:CycE}] - k_{\text{off}}[\text{Cdk2:CycE}^{\text{rem}}] - k_{\text{edeg}}[\text{Deg}][\text{Cdk2:CycE}^{\text{rem}}] + k_{\text{xdeg}}[\text{Xic:Cdk2:CycE}^{\text{rem}}] - k_{\text{assoc}}[\text{Xic}][\text{Cdk2:CycE}^{\text{rem}}] + k_{\text{dissoc}}[\text{Xic:Cdk2:CycE}^{\text{rem}}]$
6	$\frac{d}{dt}[\text{PCdk2:CycE}^{\text{rem}}] = +k_{\text{on}}\phi[\text{PCdk2:CycE}] - k_{\text{off}}[\text{PCdk2:CycE}^{\text{rem}}] - k_{\text{edeg}}[\text{Deg}][\text{PCdk2:CycE}^{\text{rem}}] + k_{\text{xdeg}}[\text{Xic:PCdk2:CycE}^{\text{rem}}] - k_{\text{assoc}}[\text{Xic}][\text{PCdk2:CycE}^{\text{rem}}] + k_{\text{dissoc}}[\text{Xic:PCdk2:CycE}^{\text{rem}}]$
7	$\frac{d}{dt}[\text{Deg*}] = k_{\text{dact}}\text{Heav}([\text{Cdk2:CycE}^{\text{rem}}] - \theta)$
8	$\frac{d}{dt}[\text{Xic}] = -k_{\text{assoc}}[\text{Xic}]([\text{Cdk2:CycE}] + [\text{PCdk2:CycE}] + [\text{Cdk2:CycE}^{\text{rem}}] + [\text{PCdk2:CycE}^{\text{rem}}]) + k_{\text{dissoc}}([\text{Xic:Cdk2:CycE}] + [\text{Xic:PCdk2:CycE}] + [\text{Xic:Cdk2:CycE}^{\text{rem}}] + [\text{Xic:PCdk2:CycE}^{\text{rem}}])$
9	$\frac{d}{dt}[\text{Xic:Cdk2:CycE}] = +k_{\text{assoc}}[\text{Xic}][\text{Cdk2:CycE}] - k_{\text{dissoc}}[\text{Xic:Cdk2:CycE}] - k_{\text{on}}\phi[\text{Xic:Cdk2:CycE}] + k_{\text{off}}[\text{Xic:Cdk2:CycE}^{\text{rem}}] - k_{\text{wee}}[\text{Wee1*}][\text{Xic:Cdk2:CycE}] + k_{25A}[\text{Xic:PCdk2:CycE}]$
10	$\frac{d}{dt}[\text{Xic:PCdk2:CycE}] = +k_{\text{assoc}}[\text{Xic}][\text{PCdk2:CycE}] - k_{\text{dissoc}}[\text{Xic:PCdk2:CycE}] - k_{\text{on}}\phi[\text{Xic:PCdk2:CycE}] + k_{\text{off}}[\text{Xic:PCdk2:CycE}^{\text{rem}}] + k_{\text{wee}}[\text{Wee1*}][\text{Xic:Cdk2:CycE}] - k_{25A}[\text{Xic:PCdk2:CycE}]$
11	$\frac{d}{dt}[\text{Xic:Cdk2:CycE}^{\text{rem}}] = +k_{\text{assoc}}[\text{Xic}][\text{Cdk2:CycE}^{\text{rem}}] - k_{\text{dissoc}}[\text{Xic:Cdk2:CycE}^{\text{rem}}] + k_{\text{on}}\phi[\text{Xic:Cdk2:CycE}] - k_{\text{off}}[\text{Xic:Cdk2:CycE}^{\text{rem}}] - k_{\text{edeg}}[\text{Deg}][\text{Xic:Cdk2:CycE}^{\text{rem}}] - k_{\text{xdeg}}[\text{Xic:Cdk2:CycE}^{\text{rem}}]$
12	$\frac{d}{dt}[\text{Xic:PCdk2:CycE}^{\text{rem}}] = +k_{\text{assoc}}[\text{Xic}][\text{PCdk2:CycE}^{\text{rem}}] - k_{\text{dissoc}}[\text{Xic:PCdk2:CycE}^{\text{rem}}] + k_{\text{on}}\phi[\text{Xic:PCdk2:CycE}] - k_{\text{off}}[\text{Xic:PCdk2:CycE}^{\text{rem}}] - k_{\text{edeg}}[\text{Deg}][\text{Xic:PCdk2:CycE}^{\text{rem}}] - k_{\text{xdeg}}[\text{Xic:PCdk2:CycE}^{\text{rem}}]$
13	$\frac{d}{dt}[\text{Xic}^{\text{rem}}] = +k_{\text{edeg}}[\text{Deg}][\text{Xic:Cdk2:CycE}^{\text{rem}}] + k_{\text{edeg}}[\text{Deg}][\text{Xic:PCdk2:CycE}^{\text{rem}}] - k_{\text{xdeg}}[\text{Xic}^{\text{rem}}]$

All concentration variables are expressed in arbitrary units, i.e. they are dimensionless numbers. Hence, all rate constants (k values) have units time^{-1}. In the text, 1 AU of Xic and CycE concentration is estimated to be approximately 33 nM. $\phi = \frac{\varepsilon + [\text{Pool}]^n}{L^n + [\text{Pool}]^n}$, $\text{Heav}(x) = \{0,\ \text{if}\ x < 0;\ 1,\ \text{if}\ x \geq 0\}$. $[\text{Pool}] = [\text{Cdk2:CycE}^{\text{rem}}] + [\text{PCdk2:CycE}^{\text{rem}}] + [\text{Xic:Cdk2:CycE}^{\text{rem}}] + [\text{Xic:PCdk2:CycE}^{\text{rem}}]$. ϕ is a Hill function describing the cooperativity of Cdk2:CycE removal. It depends on [Pool], the 'total pool' of removed cyclin E. Heav(x) is the Heaviside function, a common mathematical expression for a switch. θ is the threshold Cdk2 activity for turning on the switch. The activation kinetics of Wee1 and Kin are assumed to be zero-order ultrasensitive switches [51].

Table 3
Basal parameter values for the differential equations in Table 1

Rate constants (min^{-1})
$k_{wee}=1.5$, $k_{25A}=0.1$, $k_{on}=0.02$, $k_{off}=0.0001$, $k_{assoc}=0.1$, $k_{dissoc}=0.001$, $k_{wact}=0.75$, $k_{winact}=1.5$, $k_{iact}=0.15$, $k_{iinact}=0.6$, $k_{edeg}=0.017$, $k_{xdeg}=0.01$, $k_{dact}=0.023$
Other constants (dimensionless)
$J_{wact}=0.01$, $J_{winact}=0.01$, $J_{iact}=0.01$, $J_{iinact}=0.01$, $\theta=0.3$, $\varepsilon=0.001$, $L=0.4$, $n=4$, $[Wee1_{total}]=8$
Initial concentrations (arbitrary units)
[Cdk2:CycE] = 0.06, [PCdk2:CycE] = 0.94, [Wee1*] = 1.02, [Kin*] = 0.60, [Deg*] = 0, [all 'removed' forms] = 0, [all Xic-bound forms] = 0, [Xic] = adjustable

post-fertilization [25,32] occur, even when embryos are treated with cycloheximide to block protein synthesis, a critical constraint from the experimental literature [25].

4.3.2. Exogenous Δ34Xic1 is degraded prior to the disappearance of cyclin E

A major challenge in developing the model was the experimental result that embryos microinjected with Δ34Xic1 eventually degrade cyclin E, with a delay of only several hours [25]. If cyclin E degradation were intrinsically linked to cyclin E/Cdk2 activity as we assume, and if Δ34Xic1 inhibits cyclin E/Cdk2 activity by more than 90% [25], then cyclin E levels might persist indefinitely in Δ34Xic1-injected embryos. That this is not the case suggests that Xic1 is eventually lost from the treated embryos. In the model, we assume that Xic1 bound to the removed forms of cyclin E/Cdk2 is subject to steady degradation. Simulations show that this reasonable assumption is sufficient to account for Xic1 and cyclin E fates in treated embryos (Fig. 6). To simulate the effect of injecting Δ34Xic1, the initial concentration of Xic1 in the model was set to 3. {In simulations of unperturbed embryos (Fig. 5), [total Xic1] = 0, based on the data of [33,50].} Simulations indicate that most cyclin E/Cdk2 associates with Xic1, and this complex gradually shifts to the pool of removed forms, peaking approximately 7 h pf (Fig. 6a). Once in the removed pool, Xic1 is degraded there, consistent with experiments in egg extracts

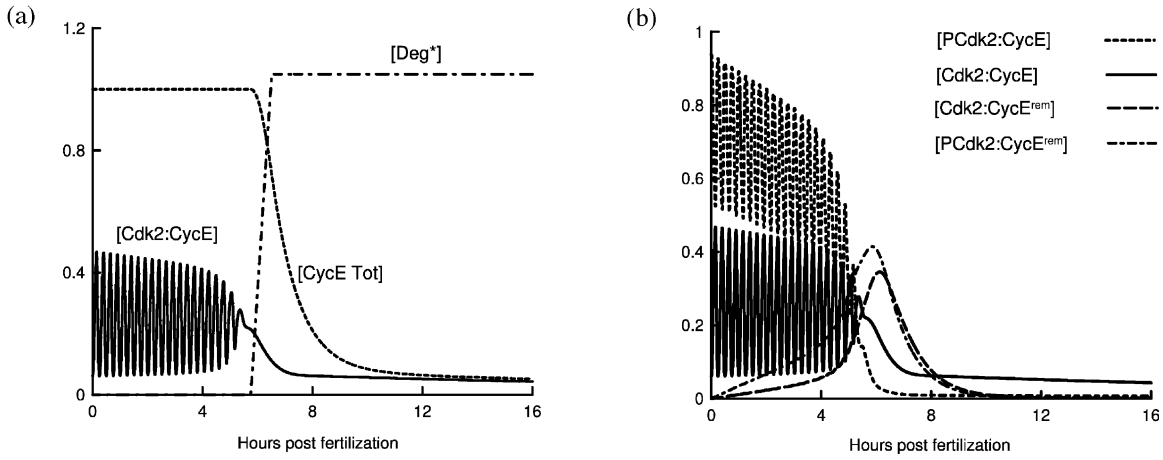

Fig. 5. The mathematical model is consistent with the dynamics observed for cyclin E/Cdk2 in normal frog embryos. (a) Numerical simulation of the equations in Table 2, given the parameter values in Table 3. The control system exhibits rapid oscillations in Cdk2 activity (period approx. 15 min) followed by abrupt degradation of cyclin E at approximately 6 h pf. (b) The four forms of cyclin E/Cdk2.

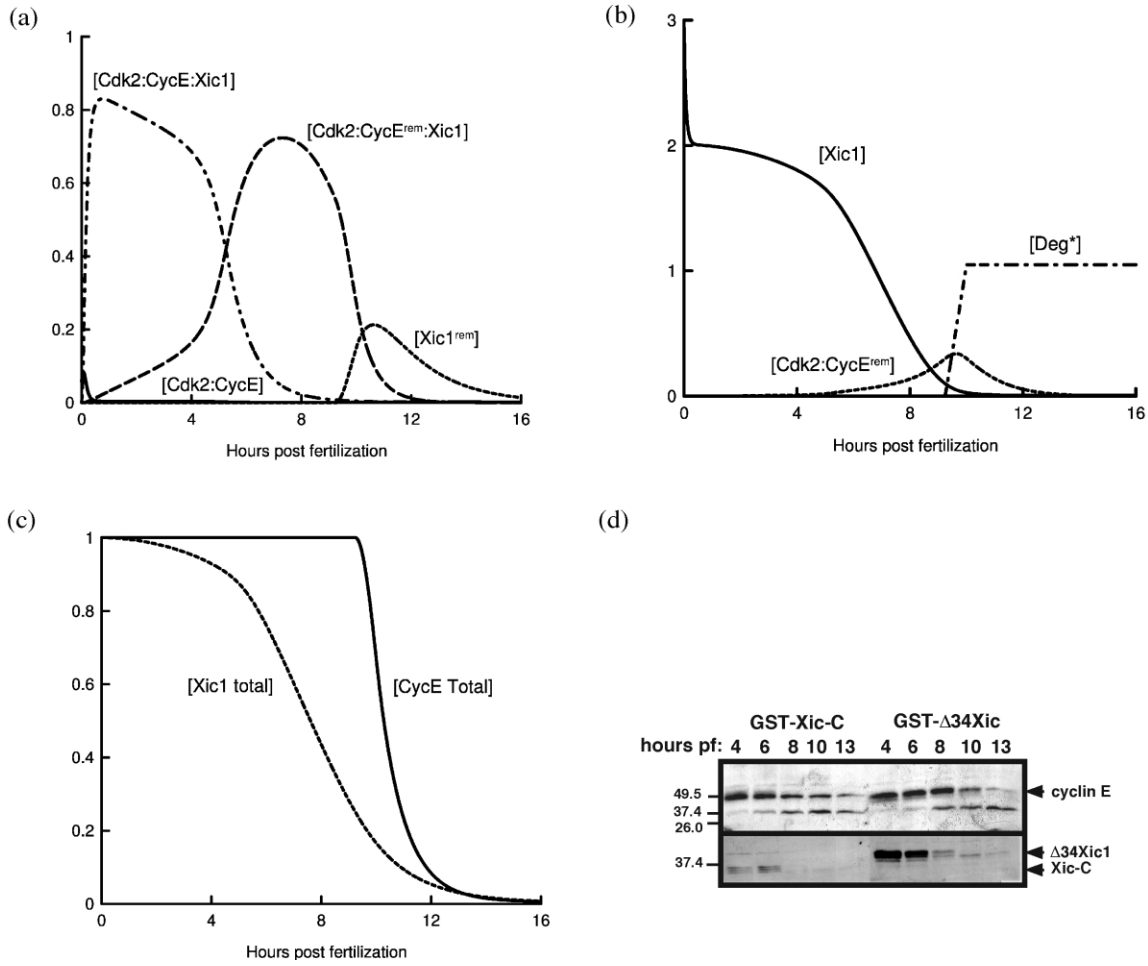

Fig. 6. Exogenous Δ34Xic1 is degraded prior to the destruction of cyclin E. (a,b,c) Simulation. $[Xic1]_{initial} = 3$. In panel (c), $[Xic1_{total}]/[Xic1]_{initial}$ is plotted. (d) Experiments. Embryos were injected with 5 ng of Xic1-C or Δ34Xic1, collected at the indicated time points and analyzed by immunoblotting for content of cyclin E and Xic1. The migration of molecular weight standards is indicated on the left. *Note*: Xic1-C reacts weakly with the Xic1 antibody, but is detected and is degraded at the same time as Δ34Xic1.

[44,45]. As long as free Xic1 is present in the cell, cyclin E/Cdk2 complexes that lose their Xic1 partner will quickly pick up another. Between 5 and 9 h, a steady drop in concentration of free Xic1 is observed, with only a modest rise in removed cyclin E/Cdk2 (Fig. 6b). Once the supply of Xic1 is exhausted, the unphosphorylated form of removed cyclinE/Cdk2 can turn on Deg (Fig. 6b) and cyclin E is degraded (Fig. 6c). We assume that removed cyclin E/Cdk2 is not immunoprecipitated and detected in H1 kinase assays because we do not detect a transient peak in cyclin E/Cdk2 activity between the degradation of microinjected Δ34Xic1 and the degradation of cyclin E (Fig. 2 and data not shown). Alternatively, the peak in removed cyclin E/Cdk2 may be too transient or too low in amplitude to be detected in our kinase assays.

Plotting levels of Δ34Xic1 and cyclin E over time (Fig. 6c) indicates that (1) cyclin E is

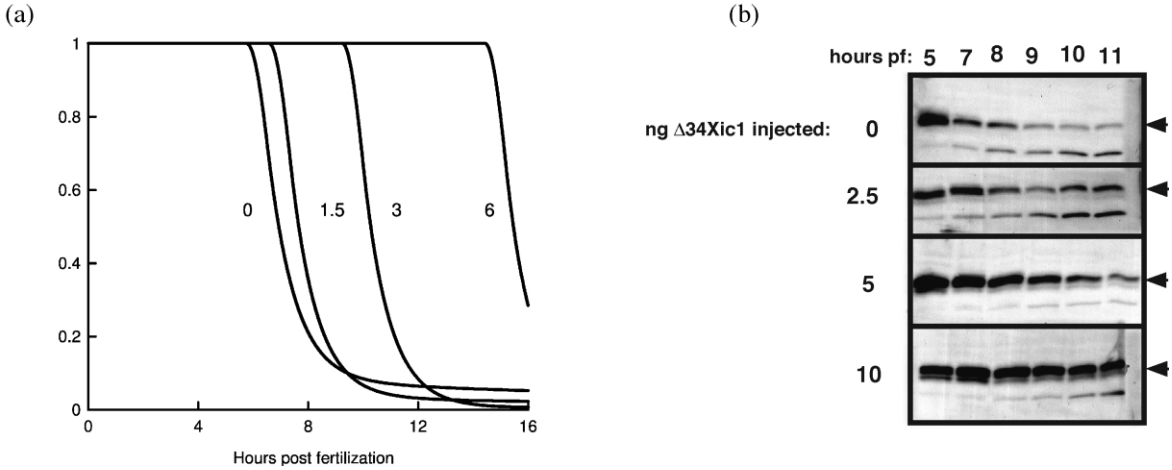

Fig. 7. Timing of cyclin E degradation is dependent upon the dose of Δ34Xic1. (a) Simulation. Total cyclin E for different amounts of Xic1 added to the system. As in Fig. 6, Xic1 is degraded prior to cyclin E. The times when one-half of the original Xic1 has been degraded are 6.4, 7.6 and 10 h for $[\text{Xic1}]_{\text{initial}} = 1.5$, 3 and 6, respectively The times when one-half of the original cyclin E has been degraded are 7, 7.7, 10.3 and 15.4 h for $[\text{Xic1}]_{\text{initial}} = 0$, 1.5, 3 and 6, respectively. (b) Experiment. Embryos were injected with 0, 2.5, 5 or 10 ng of Δ34Xic1, collected at the time points indicated, and analyzed by immunoblotting for content of cyclin E. Arrows denote the position of cyclin E.

degraded abruptly at approximately 10 h pf, consistent with observations [25], and (2) Δ34Xic1 is degraded a few hours before cyclin E.

Since the content of Δ34Xic1 over time had not been monitored in previous studies of Δ34Xic1-injected embryos, the theoretical prediction that Δ34Xic1 would be degraded prior to the degradation of cyclin E was tested experimentally. Embryos were injected with 5 ng of Xic1-C or Δ34Xic1 at the one-cell stage, collected at multiple time points and analyzed for content of cyclin E and Xic1 (Fig. 6d). The level of Δ34Xic1 dropped sharply between 6 and 8 h pf, prior to the degradation of cyclin E between 8 and 10 h pf, confirming this prediction of the model.

4.3.3. Cyclin E degradation is progressively delayed by increasing amounts of Δ34Xic1

As a final test of the model, the dose of Δ34Xic1 was altered in simulations to determine the effect on cyclin E degradation. Simulations (Fig. 7a) suggested that the timing of cyclin E degradation should be inversely correlated to the quantity of Δ34Xic1 injected over at least a four-fold range. To test this prediction experimentally, embryos were injected with 0, 2.5, 5 or 10 ng of Δ34Xic1. The total injection volume was kept constant. Embryos were analyzed for the degradation of cyclin E at multiple time points (Fig. 7b). In embryos lacking Δ34Xic1, most cyclin E degradation occurred between 5 and 7 h pf. In embryos injected with 2.5 or 5 ng of Δ34Xic1, cyclin E degradation occurred 7–8 and 9–10 h pf, respectively. Little degradation of cyclin E was detected in embryos injected with 10 ng of Δ34Xic1, even as late as 11 h pf. The simulations and experimental data correlate well, further supporting the theoretical basis of the model.

These observations allow us to estimate the 'arbitrary units' of Xic1 concentration in the model. [Total Xic1] = 1 AU corresponds to 1.67 ng of Δ34Xic1 per embryo (1.5 AU simulates activity of 2.5 ng of Δ34Xic1; 3 AU simulates 5 ng of Δ34Xic1, etc.), which is a concentration of approximately 33 nM (assuming one embryo is equivalent to 1.0 μl and the molecular weight of Δ34Xic1 is 50 000 g/mol). Since Xic1 and cyclin E/Cdk2 bind in 1:1 stoichiometry, this means that [total

cyclin E] = 1 AU also corresponds to approximately 33 nM.

5. Discussion

By combining computational and experimental approaches, we have built a model of the cyclin E/Cdk2 developmental timer in early *Xenopus* embryos. Development of the model was constrained by experimental evidence obtained from intact *Xenopus* embryos: (1) oscillations in cyclin E/Cdk2 occur twice per cell cycle prior to the MBT [25]; (2) the level of cyclin E remains constant during this time [25,32]; and (3) cyclin E is degraded at a fixed time post-fertilization, independent of cell number, protein synthesis, nucleocytoplasmic ratio and zygotic transcription [25,32]. The model faithfully reproduces 22 oscillations in cyclin E/Cdk2 activity and degradation of cyclin E at approximately 6–7 h pf, independent of protein synthesis. Experimental evidence that the degradation of cyclin E is delayed in embryos microinjected with 5 ng of Δ34Xic1 [25] also agrees with the simulations.

The model is composed of three 'modules': an oscillatory module, based on a delayed negative feedback loop; a switching module, based on cooperative removal of cyclin E/Cdk2; and a proteolysis module, based on irreversible activation of the cyclin E degradation pathway.

5.1. Oscillatory module

In the oscillatory module, oscillations in cyclin E/Cdk2 activity do not depend on cyclin E synthesis or degradation, because total cyclin E level is quite constant throughout the early stages of frog embryogenesis [25]. Nor are these oscillations attributable to periodic fluctuations in a stoichiometric inhibitor, Xic1, because Xic1 is not normally present in the early embryo [33]. That leaves reversible inhibitory phosphorylation of Cdk2 as the prime suspect for generating oscillations in cyclin E/Cdk2 activity. To the best of our knowledge, oscillations in the phosphorylation state of Cdk2 have not been measured in intact embryos and may be difficult to observe because the oscillations are rapid and may be localized within nuclei. On the other hand, Cdk2 activity is regulated by reversible phosphorylation in extracts [37], and embryos microinjected with XChk1, which promotes tyrosine phosphorylation of Cdks, have reduced cyclin E/Cdk2 activity [40]. If cyclin E/Cdk2 oscillations derive from reversible phosphorylation alone, then the components must be involved in a negative feedback loop, with cyclin E/Cdk2 either promoting Wee1 activity or inhibiting Cdc25. This supposition is in sharp contrast to the case of cyclin B/Cdk1, which inhibits Wee1 and activates Cdc25. In that case, oscillations depend on Cdk1 turning on cyclin B degradation by activating Fizzy/APC [12]. Therefore, Cdk2 oscillations are fundamentally different from Cdk1 oscillations.

At this point, the oscillatory module in Fig. 4 is purely hypothetical and awaits experimental validation. It should also be kept in mind that a negative feedback loop, whereby cyclin E/Cdk2 indirectly *inhibits* Cdc25, might be an alternative basis for oscillations in Cdk2 activity.

5.2. Switching module

The second major assumption in the model is that the timing of cyclin E degradation depends upon cyclin E/Cdk2 activity, in particular upon removed cyclin E/Cdk2. In support of this assumption, degradation of cyclin E is delayed when Cdk2 activity is inhibited by either Δ34Xic1 [25] or XChk1 (Fig. 1). However, in Δ34Xic1-injected embryos, cyclin E is eventually degraded. The model incorporates the idea that cyclin E/Cdk2 promotes chromatin association and subsequent degradation of Xic1, as suggested by the experiments of Furstenthal et al. [45]. In simulations of Δ34Xic1-injected embryos, cyclin E is degraded some hours after degradation of Δ34Xic1 (Fig. 6c). This prediction was validated experimentally (Fig. 6d).

Initially, we assumed that 'removed' cyclin E was chromatin-bound cyclin E, and that association of cyclin E with chromatin was cooperative. This assumption was based on data indicating that cyclin E/Cdk2 associates with chromatin [47] and is responsible for loading Xic1 onto chromatin, where Xic1 is then degraded [44,45]. However,

Table 4
Differential equations used for bifurcation analysis in Fig. 8

1	$\frac{d}{dt}[\text{Cdk2:CycE}] = -k_{\text{wee}}[\text{Wee1*}][\text{Cdk2:CycE}] + k_{25A}(E_{\text{tot}} - H - [\text{Cdk2:CycE}])$
3	$\frac{d}{dt}[\text{Wee1*}] = \frac{k_{\text{wact}}([\text{Wee1}_{\text{total}}] - [\text{Wee1*}])}{J_{\text{wact}} + [\text{Wee1}_{\text{total}}] - [\text{Wee1*}]} - \frac{k_{\text{winact}}[\text{Kin*}][\text{Wee1*}]}{J_{\text{winact}} + [\text{Wee1*}]}$
4	$\frac{d}{dt}[\text{Kin*}] = \frac{k_{\text{iact}}(1 - [\text{Kin*}])}{J_{\text{iact}} + 1 - [\text{Kin*}]} - \frac{k_{\text{iinact}}[\text{Cdk2:CycE}][\text{Kin*}]}{J_{\text{iinact}} + [\text{Kin*}]}$
5	$\frac{d}{dt}H = +k_{\text{on}}\frac{\varepsilon + H^n}{L^n + H^n} \times (E_{\text{tot}} - H) - k_{\text{off}}H$

In the simplified model, cyclin E degradation and Xic1 binding are ignored. These equations are carried over from Table 2, with the understanding that H = [removed forms of Cdk2:CycE] and E_{tot} = [all forms of Cdk2:CycE].

binding of cyclin E/Cdk2 to chromatin depends upon DNA replication cycles [47], inconsistent with observations that degradation of cyclin E occurs at a fixed time, even in cycloheximide-treated embryos (in which DNA replication is blocked indirectly) [25,41]. Therefore, we abandoned the specific model of chromatin binding.

Alternatively, 'removed' cyclin E/Cdk2 could be a posttranslationally modified form. When cyclin E is autophosphorylated by cyclin E/Cdk2, it binds an F-box protein and becomes ubiquitinated and degraded by the SCF (reviewed in [48]). If autophosphorylated cyclin E/Cdk2 were rapidly degraded, then the removal step would not be cooperative. Therefore, a sufficient time delay is needed between autophosphorylation and degradation of cyclin E. Since cyclin E needs to be phosphorylated at a second site prior to degradation [49], the time delay could exist if autophosphorylated cyclin E/Cdk2 were to phosphorylate and activate another kinase (e.g. Deg). One discrepancy with our model is that Xic should inhibit the removal of cyclin E in this case, since 'removal' depends upon cyclin E/Cdk2 catalytic activity. A key assumption of the model is that removal is not inhibited by Xic. Clearly, the details of the removal step are speculative and need to be determined by future experimentation. Therefore, the removal mechanism remains deliberately general in the model.

5.3. Degradation module

We have not attempted to model the molecular machinery of cyclin E degradation, because it does not feedback, as far as we know, on the dynamics of the oscillatory and switching modules. To keep this part of the model as simple as possible, we use a 'Heaviside function' to switch on cyclin E degradation in an irreversible fashion, after a sufficient amount of Cdk2:CycE^{rem} has accumulated.

5.4. Bifurcation analysis of the mathematical model

To understand better the fundamental behavior of the cyclin E/Cdk2 developmental timer, bifurcation analysis was applied to a simplified version of the model. (A primer on bifurcation analysis is available in [15].) Because our aim was to uncover the dynamics of the oscillatory and switching modules, we have eliminated Xic1 binding and cyclin E degradation from the network (see Table 4). A numerical simulation of these equations is presented in Fig. 8a. Removed cyclin E/Cdk2 (*dashed line*) increases abruptly at approximately 6 h pf, indicative of cooperativity, as postulated by the model. Oscillations in active free cyclin E/Cdk2 (*solid line*) are created by the negative feedback loop involving Wee1 and quenched by the cooperative removal of cyclin E/Cdk2.

In Fig. 8b, we consider the behavior of the negative feedback loop as a function of the fraction of removed cyclin E. That is, we fix [Cdk2:CycE^{rem}] + [PCdk2:CycE^{rem}] = H = constant, and study the behavior of the negative feedback loop as a function of the value of H. For $0 < H < 0.45$, the steady-state solution of the negative feedback

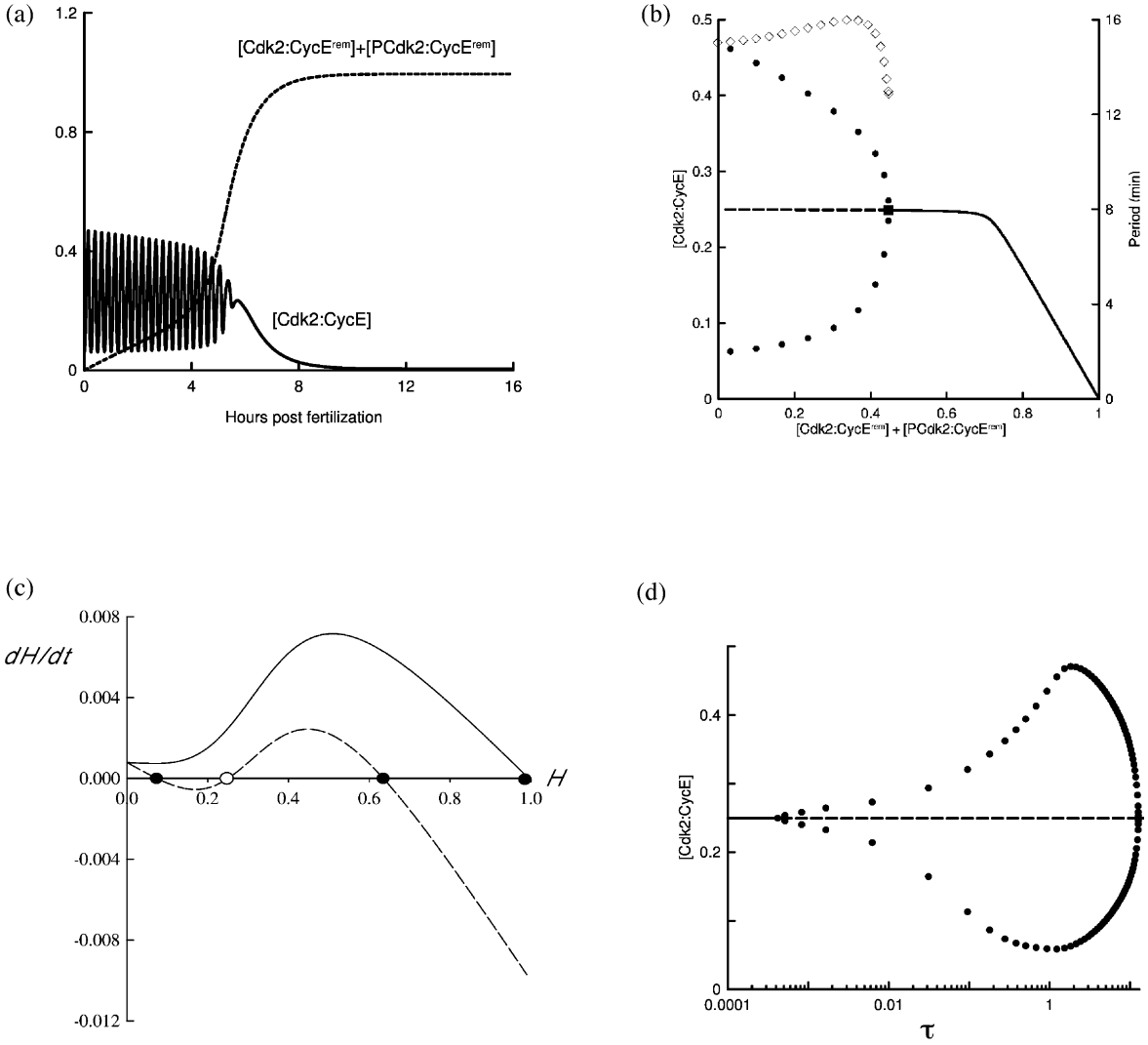

Fig. 8. Bifurcation analysis of the cyclin E/Cdk2 developmental timer. (a) Simulation of the equations in Table 4. Removed cyclin E/Cdk2 (*dashed line*; $H = [\text{Cdk2:CycE}^{\text{rem}}] + [\text{P Cdk2:CycE}^{\text{rem}}]$) and active, unremoved cyclin E/Cdk2 (*solid line*) as functions of time. (b) Dependence of negative feedback oscillations on H. The ordinate is [Cdk2:CycE], except for the open diamonds, which indicate the period of oscillation (scale on right). Solid line, stable steady state; dashed line, unstable steady state; black circles, maximum and minimum values of [Cdk2:CycE] during the course of an oscillation at fixed H. The control system undergoes a Hopf bifurcation at $H = 0.45$. (c) Bistability in the positive feedback module. We plot dH/dt as a function of H for two values of k_{off}. The system is monostable (one steady state, where $dH/dt = 0$) for $k_{\text{off}} = 0.0001$ (*solid line*) and bistable (three steady states) for $k_{\text{off}} = 0.01$ (*dashed line*). (d) Oscillations in the negative feedback module, $H = 0$. Symbols as in panel (b). The steady state is unstable between the two points of Hopf bifurcation at $\tau = 4 \times 10^{-4}$ and 12 (see text).

loop (*dashed line*) is unstable, and the network executes sustained oscillations (the black circles indicate the maximum and minimum values of active cyclin E/Cdk2 over the course of an oscillation) with period close to 14 min (*open diamonds*). For $0.45 < H < 1$, the negative feedback loop has a stable steady state (*solid line*) and no sustained oscillations. At $H = 0.45$, the negative

feedback loop is said to undergo a Hopf bifurcation. Now, comparing Fig. 8a,b, we observe that as H increases from 0 to 0.45 (during the first 5 h pf), the negative feedback loop oscillates with a period of approximately 14 min. However, as soon as H exceeds the Hopf-bifurcation point, the oscillations are quickly lost.

To see why H increases as in Fig. 8a, we plotted the rate of change of H (dH/dt) as a function of H in Fig. 8c. When dH/dt is positive, H increases; when dH/dt is negative, H decreases. Steady states exist wherever $dH/dt=0$. For the parameter set used here (*solid line*), a single stable steady state exists at H close to 1. Hence, starting with $H=0$ (no removed cyclin E/Cdk2), H must increase until it reaches the steady state, where most cyclin E/Cdk2 is removed. Note, however, that the rate of increase of H is, at first, very small ($dH/dt \approx 0.0008$) and then accelerates rapidly by nearly 10-fold. This acceleration is a reflection of the cooperative removal of cyclin E/Cdk2 in the model.

Cooperative removal is a form of positive feedback (autocatalysis) that can easily create bistable behavior. If the dissociation rate constant, k_{off}, is increased from 0.0001 to 0.01, then dH/dt as a function of H is modified (*dashed line*) so that there now exist two stable steady states: one with $H \approx 0.1$ (little removed cyclin E), and another with $H \approx 0.7$ (most cyclin E removed). At the lower steady state, the negative feedback loop will be in its oscillatory regime, and at the upper steady state, the negative feedback loop will be quiescent. This behavior of the control system is entirely different from what is observed. We have chosen our parameter set (Table 3) to bring the control system close to but not within its region of bistability. With this choice, H increases slowly at first, pulling the oscillatory module past its Hopf bifurcation, and then H increases rapidly, as most of the cyclin E is removed from the oscillatory system.

Finally, we have mentioned several times that oscillations in the negative feedback loop require an intermediate, Kin, between cyclin E/Cdk2 and Wee1. Kin introduces a time delay between activation of cyclin E/Cdk2 and subsequent increase in Wee1 activity. This time delay depends on the characteristic time, τ, required for cyclin E/Cdk2 to inactivate Kin ($\tau = 1/k_{iinact}$). The basal value of τ is 1.67 (see Table 3). As τ decreases, the time delay in the negative feedback loop becomes negligible, and oscillations disappear at a Hopf bifurcation, at $\tau = 4 \times 10^{-4}$ in Fig. 8d. (To keep the relative activity of Kin fixed, we steadily increase both k_{iact} and k_{iinact}, keeping their ratio constant at $k_{iact}/k_{iinact} = 0.25$.) The amplitude of oscillation becomes quite small, even for $\tau < 0.05$. In other words, oscillations in the negative feedback loop require an intermediate that introduces a minimal time lag between cyclin E/Cdk2 and Wee1. Fig. 8d shows that oscillations are also lost if τ becomes too large ($\tau > 12$).

5.5. Future developments

The model presented here will be refined as new experimental data become available. Most importantly, experiments are needed to identify whether Kin exists and functions in a negative feedback loop between cyclin E/Cdk2 and Wee1. Alternatively, does negative feedback exist between cyclin E/Cdk2 and Cdc25? In addition, the specific nature of 'removed' cyclin E needs to be determined.

Acknowledgments

We are grateful to Dr Rebecca Hartley (University of New Mexico Health Sciences Center) for the cyclin E antibody, and to Dr James Maller (Howard Hughes Medical Institute, University of New Mexico Health Sciences Center) for the Xic1 protein and cyclin antibodies. The experiment in Fig. 1 was performed by JCS while in Dr Maller's lab. We appreciate Dr Monica Murakami's (National Cancer Institute; NIH) help with preliminary Wee1 studies. This work has been supported by the National Institutes of Health (Grant Numbers R01-GM59688 to JCS, R01-GM64339 to JJT), the Defense Advanced Research Projects Agency—Biocomputation Program (AFRL #F30602-02-0572), the National Science Foundation—Biocomplexity Program (MCB-0083315), and the Research Division of Virginia Tech.

References

[1] M.J. Solomon, M. Glotzer, T.H. Lee, M. Phillippe, M.W. Kirschner, Cyclin activation of $p34^{cdc2}$, Cell 63 (1990) 1013–1024.

[2] M.J. Solomon, T.H. Lee, M.W. Kirschner, Role of phosphorylation in $p34^{cdc2}$ activation: identification of an activating kinase, Mol. Cell. Biol. 3 (1992) 13–27.

[3] A.W. Murray, M.W. Kirschner, Cyclin synthesis drives the early embryonic cell cycle, Nature 339 (1989) 275–280.

[4] A. Devault, D. Fesquet, J.-C. Cavadore, et al., Cyclin A potentiates maturation-promoting factor activation in the early *Xenopus* embryo via inhibition of the tyrosine kinase that phosphorylates cdc2, J. Cell Biol. 118 (1992) 1109–1120.

[5] P.R. Mueller, T.R. Coleman, W.G. Dunphy, Cell cycle regulation of a *Xenopus* Wee1-like kinase, Mol. Biol. Cell 6 (1995) 119–134.

[6] P.R. Mueller, T.R. Coleman, A. Kumagai, W.G. Dunphy, Myt1: a membrane-associated inhibitory kinase that phosphorylates cdc2 on both threonine-14 and tyrosine-15, Science 270 (1995) 86–90.

[7] J. Gautier, M.J. Solomon, R.N. Booher, J.F. Bazan, M.W. Kirschner, cdc25 is a specific tyrosine phosphatase that directly activates $p34^{cdc2}$, Cell 67 (1991) 197–211.

[8] A. Kumagai, W.G. Dunphy, The cdc25 protein controls tyrosine dephosphorylation of the cdc2 protein in a cell-free system, Cell 64 (1991) 903–914.

[9] A. Kumagai, W.G. Dunphy, Regulation of the cdc25 protein during the cell cycle in *Xenopus* extracts, Cell 70 (1992) 139–151.

[10] C. Smythe, J.W. Newport, Coupling of mitosis to the completion of S-phase in *Xenopus* occurs via modulation of the tyrosine kinase that phosphorylates $p34^{cdc2}$, Cell 68 (1992) 787–797.

[11] T. Izumi, J.L. Maller, Elimination of cdc2 phosphorylation sites in the cdc25 phosphatase blocks initiation of M-phase, Mol. Biol. Cell 4 (1993) 1337–1350.

[12] T. Lorca, A. Castro, A.M. Martinez, et al., Fizzy is required for activation of the APC/cyclosome in *Xenopus* egg extracts, EMBO J. 17 (1998) 3565–3575.

[13] B. Novak, J.J. Tyson, Numerical analysis of a comprehensive model of M-phase control in *Xenopus* oocyte extracts and intact embryos, J. Cell Sci. 106 (1993) 1153–1168.

[14] B. Novak, J.J. Tyson, Quantitative analysis of a molecular model of M-phase control in *Xenopus* oocyte extracts and intact embryos, J. Theor. Biol. 173 (1995) 283–305.

[15] M.T. Borisuk, J.J. Tyson, Bifurcation analysis of a model of mitotic control in frog eggs, J. Theor. Biol. 195 (1998) 69–85.

[16] G. Marlovits, C.J. Tyson, B. Novak, J.J. Tyson, Modeling M-phase control in *Xenopus* oocyte extracts: the surveillance mechanism for unreplicated DNA, Biophys. Chem. 72 (1998) 169–184.

[17] M.A. Felix, J.C. Labbe, M. Doree, T. Hunt, E. Karsenti, Triggering of cyclin degradation in interphase extracts of amphibian eggs by cdc2 kinase, Nature 346 (1990) 379–382.

[18] Y. Masui, C. Markert, Cytoplasmic control of nuclear behavior during meiotic maturation of frog oocytes, J. Exp. Zool. 177 (1971) 129–146.

[19] J. Gerhart, M. Wu, M. Kirschner, Cell cycle dynamics of an M-phase-specific cytoplasmic factor in *Xenopus laevis* oocytes and eggs, J. Cell. Biol. 98 (1984) 1247–1255.

[20] M. Cyert, M. Kirschner, Regulation of MPF activity in vitro, Cell 53 (1988) 185–195.

[21] A. Kumagai, W.G. Dunphy, Regulation of *Xenopus* cdc25 protein, Methods Enzymol. 283 (1997) 564–571.

[22] J. Newport, M. Kirschner, A major developmental transition in early *Xenopus* embryos: I. Characterization and timing of cellular changes at the midblastula stage, Cell 30 (1982) 675–686.

[23] J. Newport, M. Kirschner, A major developmental transition in early *Xenopus* embryos: II. Control of the onset of transcription, Cell 30 (1982) 687–696.

[24] D.L. Frederick, M.T. Andrews, Cell cycle remodeling requires cell–cell interactions in developing *Xenopus* embryos, J. Exp. Zool. 270 (1994) 410–416.

[25] R.S. Hartley, J.C. Sible, A.L. Lewellyn, J.L. Maller, A role for cyclin E/Cdk2 in the timing of the midblastula transition in *Xenopus* embryos, Dev. Biol. 188 (1997) 312–321.

[26] R.S. Hartley, R.E. Rempel, J.L. Maller, In vivo regulation of the early embryonic cell cycles in *Xenopus*, Dev. Biol. 173 (1996) 408–419.

[27] P.K. Jackson, S. Chevalier, M. Philippe, M.W. Kirschner, Early events in DNA replication require cyclin E and are blocked by $p21^{CIP1}$, J. Cell Biol. 130 (1995) 755–769.

[28] U.P. Strausfeld, M. Howell, R. Rempel, J.L. Maller, T. Hunt, J.J. Blow, Cip1 blocks the initiation of DNA replication in *Xenopus* extracts by inhibition of cyclin-dependent kinases, Curr. Biol. 4 (1994) 876–883.

[29] E.H. Hinchcliffe, C. Li, E.A. Thompson, J.L. Maller, G. Sluder, Requirements of Cdk2-cyclin E activity of repeated centrosome reproduction in *Xenopus* egg extract, Science 283 (1999) 851–854.

[30] K.R. Lacey, P.K. Jackson, T. Stearns, Cyclin-dependent kinase control of centrosome duplication, Proc. Natl. Acad. Sci. USA 96 (1999) 2817–2822.

[31] R.E. Rempel, S.B. Sleight, J.L. Maller, Maternal *Xenopus* Cdk2–cyclin E complexes function during meiotic and early embryonic cell cycles that lack a G1-phase, J. Biol. Chem. 270 (1995) 6843–6855.

[32] J.A. Howe, J.W. Newport, A developmental timer regulates degradation of cyclin E1 at the midblastula

transition during *Xenopus* embryogenesis, Proc. Natl. Acad. Sci. USA 93 (1996) 2060–2064.

[33] W. Shou, W.G. Dunphy, Cell cycle control by *Xenopus* $p28^{Kix1}$, a developmentally regulated inhibitor of cyclin-dependent kinases, Mol. Biol. Cell 7 (1996) 457–469.

[34] A.W. Murray, M.J. Solomon, M.W. Kirschner, The role of cyclin synthesis and degradation in the control of maturation promoting factor activity, Nature 339 (1989) 280–286.

[35] J.E. Ferrell, M. Wu, J.C. Gerhart, G.S. Martin, Cell cycle tyrosine phosphorylation of $p34^{cdc2}$ and a microtubule-associated protein kinase homolog in *Xenopus* oocytes and eggs, Mol. Cell. Biol. 11 (1991) 1965–1971.

[36] S. Kim, C. Li, J. Maller, A maternal form of the phosphatase Cdc25A regulates early embryonic cell cycles in *Xenopus laevis*, Dev. Biol. 212 (1999) 381–391.

[37] V. D'Angiolella, V. Costanzo, M.E. Gottesman, E.V. Avvedimento, J. Gautier, D. Grieco, Role for cyclin-dependent kinase 2 in mitosis exit, Curr. Biol. 11 (2001) 1221–1226.

[38] P.D. Nieuwkoop, J. Faber, Normal Table of *Xenopus laevis*, North Holland Publishing Company, Amsterdam, 1975.

[39] J.-Y. Su, R.E. Rempel, E. Erikson, J.L. Maller, Cloning and characterization of the *Xenopus* cyclin-dependent kinase inhibitor $p27^{Xic1}$, Proc. Natl. Acad. Sci. USA 92 (1995) 10187–10191.

[40] N. Kappas, P. Savage, K.C. Chen, A.T. Walls, J.C. Sible, Dissection of the XChk1 signaling pathway in *Xenopus laevis* embryos, Mol. Biol. Cell 11 (2000) 3101–3108.

[41] J.C. Sible, J.A. Anderson, A.L. Lewellyn, J.L. Maller, Zygotic transcription is required to block a maternal program of apoptosis in *Xenopus* embryos, Dev. Biol. 189 (1997) 335–346.

[42] J.J. Tyson, B. Novak, G.M. Odell, K. Chen, C.D. Thron, Chemical kinetic theory: understanding cell–cycle regulation, Trends Biochem. Sci. 21 (1996) 89–96.

[43] J.S. Griffith, Mathematics of cellular control processes. I. Negative feedback to one gene, J. Theor. Biol. 20 (1968) 202–208.

[44] C. Swanson, J. Ross, P.K. Jackson, Nuclear accumulation of cyclin E/Cdk2 triggers a concentration-dependent switch for the destruction of $p27^{Xic1}$, Proc. Natl. Acad. Sci. USA 97 (2000) 7796–7801.

[45] L. Furstenthal, C. Swanson, B.K. Kaiser, A.G. Eldridge, P.K. Jackson, Triggering ubiquitination of a CDK inhibitor at origins of replication, Nat. Cell Biol. 3 (2001) 715–722.

[46] L.-C. Chuang, P.R. Yew, Regulation of nuclear transport and degradation of the *Xenopus* cyclin-dependent kinase inhibitor, $p27^{Xic1}$, J. Biol. Chem. 276 (2001) 1610–1617.

[47] L. Furstenthal, B. Kaiser, C. Swanson, P. Jackson, Cyclin E uses Cdc6 as a chromatin-associated receptor required for DNA replication, J. Cell Biol. 152 (2001) 1267–1278.

[48] J. Bartek, J. Lukas, Order from destruction, Science 294 (2001) 66–67.

[49] H. Strohmaler, C.H. Spruck, P. Kaiser, K.-A. Won, O. Sangfelt, S.I. Reed, Human F-box protein hCdc4 targets cyclin E for proteolysis and is mutated in a breast cancer cell line, Nature 413 (2001) 316–322.

[50] C.V. Finkelstein, L.G. Chen, J.L. Maller, A role for G1/S cyclin-dependent protein kinases in the apoptotic response to ionizing radiation, J. Biol. Chem. 277 (2002) 38476–38485.

[51] A. Goldbeter, D.E.J. Koshland, An amplified sensitivity arising from covalent modification in biological systems, Proc. Natl. Acad. Sci. USA 78 (1981) 6840–6844.